Product Branching Ratios of the $C(^3P) + C_2H_3(^2A')$ and $CH(^2\Pi) + C_2H_2(^1\Sigma_g^+)$ Reactions and Photodissociation of $H_2CC{\equiv}CH(^2B_1)$ at 193 and 242 nm: an ab Initio/RRKM Study

Thanh Lam Nguyen,[†] Alexander M. Mebel,*[,†] Sheng H. Lin,[†] and Ralf I. Kaiser[‡]

Institute of Atomic and Molecular Sciences, Academia Sinica, P.O. Box 23-166, Taipei 10764, Taiwan, and Department of Chemistry, University of York, York YO 10 5DD, U.K.

Received: June 5, 2001; In Final Form: August 28, 2001

The $C(^3P) + C_2H_3(^2A')$ and $CH(^2\Pi) + C_2H_2$ reactions have been studied using ab initio/RRKM calculations to investigate possible formations of C_3H_2 and C_3H isomers in extraterrestrial environments such as circumstellar envelopes of carbon stars and cold molecular clouds, combustion processes, and CVD. Microcanonical rate constants and product branching ratios have been calculated. Product branching ratios for the $C(^3P) + C_2H_3(^2A')$ are obtained as 78.3−81.8% for the $HCCCH(^3B) + H$ products, 6.1−7.3% for c-$C_3H_2(^1A_1) + H$, 4.4−8.1% for $H_2CCC(^1A_1) + H$, 5.5% for $HCCC(^2A') + H_2$, and 1.0−2.0% for the $CH(^2\Pi) + C_2H_2$ products, depending on the initial concentrations of intermediates c-H_2CCCH and $H_2CC(H)C$, both of which can be produced at the initial reaction step without entrance barrier. Thus, the $C(^3P) + C_2H_3(^2A')$ reaction can be expected to mainly produce C_3H_2 isomers in extraterrestrial environments. Product branching ratios for the $CH(^2\Pi) + C_2H_2$ reaction slightly vary with the initial concentrations of two initial complexes c-C_3H_3 and CHCHCH, which can be formed from the reactants without barriers and are calculated as 84.5−87.0% for $HCCCH(^3B) + H$, 10.2−12.8% for c-$C_3H_2(^1A_1) + H$, 1.8−1.9% for $HCCC(^2A') + H_2$, and 0.9% for $H_2CCC(^1A_1) + H$. The photodissociation of propargyl radical has been also investigated at photon energies of 193 and 242 nm, assuming internal conversion into the ground electronic state before dissociation. Product branching ratios calculated at 193 nm are 86.5% for the $HCCCH(^3B) + H$ channel, 3.6% for c-$C_3H_2(^1A_1) + H$, 5.5% for $HCCC(^2A') + H_2$, 3.5% for $H_2CCC(^1A_1) + H$, and 0.9% for $CH(^2\Pi) + C_2H_2$. These results are in line with experimental measurements (ref 24), which gave 96% and 4% branching ratios for the $C_3H_2 + H$ and $C_3H + H_2$ channels, respectively. Product branching ratios obtained at 242 nm are 90.2% for the $HCCCH(^3B) + H$ channel, 5.1% for c-$C_3H_2(^1A_1) + H$, 3.0% for $HCCC(^2A') + H_2$, 1.6% for $H_2CCC(^1A_1) + H$, and 0.1% for $CH(^2\Pi) + C_2H_2$. Thus, $HCCCH(^3B)$ and H are predicted to be the major products, while c-C_3H_2 and H are expected to play only a minor role.

1. Introduction

The singlet cyclopropenylidene isomer (c-C_3H_2, C_{2v}, $^1A_1$) was detected in the interstellar medium (ISM) in 1985 using microwave spectroscopy.[1,2] Subsequent quantitative surveys indicated that c-C_3H_2 is one of the most abundant molecules in interstellar environments, such as dark clouds TMC-1, Oph A, Ori A, and SgrB2 as well as the carbon star IRC +10216, with fractional abundances up to 10^{-8} cm^{-3}.[1−5] In diffuse clouds, cyclopropenylidene is depleted by a factor of about 100.[6] A second C_3H_2 isomer, singlet vinylidenecarbene (H_2CCC, C_{2v}, $^1A_1$), was discovered six years later by Cernicharo et al. toward TMC-1.[7] Compared to cyclopropenylidene, its fractional abundance is only 1−2%. Surprisingly, a third isomer-triplet propargylene (HCCCH, C_2, ^3B), although more stable than vinylidenecarbene, has never been observed in the ISM. The formation mechanism of these C_3H_2 isomers has not been established either experimentally or theoretically.[8] Chemical models of multiple ion−molecule reactions for the formation of C_3H_2 isomers have been suggested[9] as follows:

$$C_2H_2 + C^+ \rightarrow l/c\text{-}C_3H^+ + H \quad (1)$$

$$l/c\text{-}C_3H^+ + H_2 \rightarrow c\text{-}C_3H_3^+ + h\nu \quad (2)$$

$$l/c\text{-}C_3H_3^+ + e \rightarrow l/c\text{-}C_3H_2 + H \quad (3)$$

$$C_2H_4 + C^+ \rightarrow c\text{-}C_3H_3^+ + H \quad (4)$$

$$\rightarrow c\text{-}C_3H_2^+ + H_2 \quad (5)$$

$$\rightarrow l\text{-}C_3H_2^+ + H_2 \quad (6)$$

$$l/c\text{-}C_3H_3^+ + e \rightarrow l/c\text{-}C_3H_2 + H \quad (7)$$

The above reaction mechanism cannot account for fractional abundances, isomer-ratios of c-C_3H_2 versus H_2CCC, or for the high deuterium enrichment observed in c-C_3HD versus c-C_3H_2, i.e., an observed value of 0.08 in TMC-1 versus 0.015, as obtained in chemical models. On the other hand, the reaction of atomic carbon with vinyl radical producing C_3H_2 isomers through a single encounter can replace the ion−molecule synthesis occurring by four to five steps.

In our previous paper,[10] the potential energy surface (PES) of the $C(^3P) + C_2H_3(^2A')$ reaction was investigated at the RCCSD(T)/6-311+G(3df,2p)//B3LYP/6-311G(d,p) level of theory. We showed that C_3H_3 radicals (also thought to be of

* Corresponding author. Fax: (+886)-2-23620200. E-mail: mebel@po.iams.sinica.edu.tw.
† Academica Sinica.
‡ University of York.

10.1021/jp012129g CCC: $20.00
Published on Web 12/01/2001

major importance in formation of the first aromatic ring by recombination of two propargyl radicals, which is followed by a unimolecular rearrangement[11−22]) are produced as highly reactive intermediates, followed by splitting atomic or molecular hydrogen to produce C_3H_2 or C_3H isomers, respectively. According to our results,[10] the most energetically favorable channel is the formation of c-C_3H_2, so it can be expected to be one of the major products. Meanwhile, the other reaction channels leading to HCCCH(^{3}B), $H_2CCC(^1A_1)$, and HCCC(^{2}A′) exhibit barriers only 1−5 kcal/mol higher than those to produce c-C_3H_2. Therefore, detailed RRKM calculations are needed to predict the product branching ratios under various reaction conditions.

In this paper, we report rate constants for unimolecular steps and product branching ratios for the $C(^3P) + C_2H_3(^2A')$ reaction at a collision energy of 0.0 kcal/mol (in order to simulate the low-temperature conditions of about 10 K in cold molecular clouds), obtained using the ab initio/RRKM calculations at zero-pressure conditions. The second reaction, $CH(^2\Pi) + C_2H_2(^1\Sigma_g^+)$ occurring on the identical C_3H_3 PES, was theoretically characterized using the B3LYP/6-31G(d,p) and CASPT2 methods by Vereecken and co-workers.[23a] Kinetic calculations for this reaction over extended temperature and pressure region have been also reported recently.[23b] Earlier, Guadagnini et al.[24] carried out RRKM calculations for the $CH(^2\Pi) + C_2H_2(^1\Sigma_g^+)$ reaction using PES, which appeared to be incomplete. We computed rate constants and product branching ratios for this reaction as well, also at a collision energy of 0.0 kcal/mol, and compared our results with those of Vereecken and Peeters.[23b] Finally, we calculated product branching ratios in photodissociation of propargyl radical $H_2C-C\equiv CH(C_{2v}, {}^2B_1)$, which was experimentally studied at a photon energy of 193 nm by Jackson et al.[25] and 242 nm by Deyerl et al.,[26] assuming that photoexcitation is followed by fast internal conversion into the vibrationally hot ground electronic state and the dissociation occurs on the ground-state PES.

2. Theoretical Methods

2.1. RRKM Calculations. For a unimolecular reaction

$$R^* \rightarrow TS^{\neq} \rightarrow P$$

where R* is the energized reactant, $TS^{\neq}$ is the activated complex or transition state on the PES, and P represents product or products, the microcanonical rate constant, $k(E)$, can be expressed[27] as

$$k(E) = \frac{\sigma}{h}\frac{W^{\neq}(E - E^{\neq})}{\rho(E)}, \qquad (8)$$

according to the RRKM theory. Here σ is the symmetry factor, h is the Planck's constant, $W^{\neq}(E - E^{\neq})$ denotes the total number of states of the transition state with activation energy (barrier height) $E^{\neq}$, and $\rho(E)$ represents the density of states of the energized reactant molecule. Since we consider reactions under collision-free interstellar space or molecular beam conditions (at zero collision energy), the initial thermal distributions are assumed to be at 0 K so that the initial energy distributions are chemical activation delta functions centered at the critical energy for the respective entrance channels. The $W^{\neq}(E - E^{\neq})$ and $\rho(E)$ values can be evaluated using the saddle-point method[27] or the Whitten−Rabinovitch approximation,[28−30] which generally give similar results. Both methods are adequate as long as the chemically activated C_3H_3 does not decompose significantly via the entrance channels [$C(^3P) + C_2H_3(^2A')$ or $CH(^2\Pi) + C_2H_2(^1\Sigma_g^+)$], where these methods will be inaccurate near the reaction threshold. However, all $C_3H_2 + H$ and $C_3H + H_2$ product channels are highly exothermic making decomposition via the entrance channels unlikely. It should be mentioned that in some cases the calculated rate constants exceed 10^{13} s^{-1} and approach the applicability limit of the RRKM theory, which assumes that the species are vibrationally equilibrated, as the time scale of the vibrational relaxation normally is in the picosecond or subpicosecond range.

For some decomposition channels which do not have or have very low exit barriers on the PES, for instance, decomposition of $H_2C-C\equiv CH$ leading to $H + HCCCH(^3B)$ or $H_2CCC + H$ and dissociation of cyclic C_3H_3 (**2**) to c-$C_3H_2 + H$ and $CH + C_2H_2$, the microcanonical variational transition state theory (MVTST)[29,30] was used. The transition state position was determined based on the following criterion:

$$\frac{\partial k(E)}{\partial R_C} = 0 \text{ or } \frac{\partial W(E,R_C)}{\partial R_C} = 0 \qquad (9)$$

where W is the number of states and R_C is the reaction coordinate. The reaction coordinates were chosen as the lengths of breaking C−H bonds for the $H + HCCCH(^3B)$, c-$C_3H_2 +$ H, or $H_2CCC + H$ channels. The B3LYP/6-311G(d,p) method was used to obtain geometries along the reaction coordinates and to compute 3N-7 vibrational frequencies projected out of the gradient direction. The RCCSD(T)/6-311+G(3df,2p) method was then used to obtain more reliable energies on PES along the reaction coordinates. The Molpro 98, Molpro 2000,[31] and Gaussian 98[32] programs were employed for the calculations.

2.2. Product Branching Ratios. Under collision-free interstellar space or molecular beam conditions, master equations for unimolecular reactions can be expressed as follows:

$$\frac{d[C]_i}{dt} = \sum k_n[C]_j - \sum k_m[C]_i \qquad (10)$$

where $[C]_i$ and $[C]_j$ are concentrations of various intermediates or products and k_n and k_m are microcanonical rate constants computed using eq 8. The fourth-order Runge−Kutta method[29] was used to solve the system of eq 10. We obtained numerical solutions for concentrations of various products versus time. The concentrations at the times when they have converged were used for calculations of product branching ratios. To verify the applicability of the Runge−Kutta method for the stiffest system of differential equations (for the $CH(^2\Pi) + C_2H_2(^1\Sigma_g^+)$ reaction), we additionally solved it using the semiimplicit extrapolation method recommended in Numerical Recipes.[33] Nearly identical results were obtained.

3. Results

Table 1 contains various parameters used for the search of variational transition states, including breaking bond distances, relative energies, and vibrational frequencies. Rate constants for individual steps of the $C(^3P) + C_2H_3(^2A')$ and $CH(^2\Pi) + C_2H_2(^1\Sigma_g^+)$ reactions are collected in Tables 2 and 3, respectively, and those for photodissociation of the propargyl radical at 193 and 242 nm are compiled in Table 4. Product branching ratios for the $C(^3P) + C_2H_3(^2A')$ and $CH(^2\Pi) + C_2H_2(^1\Sigma_g^+)$ reactions are shown in Tables 5 and 6, respectively. A profile of the C_3H_3 PES constructed utilizing the RCCSD(T)/6-311+G(3df,2p)//B3LYP/6-311G(d,p) approach (see ref 10) is depicted in Figure 1. Reaction schemes chosen for kinetic calculations of the $C(^3P) + C_2H_3(^2A')$ and $CH(^2\Pi) + C_2H_2(^1\Sigma_g^+)$ reactions

TABLE 1: Breaking Bond Distances (R_C, in Å), Relative Energies (E, in kcal/mol), and Frequencies (ν_i, in cm^{-1}) for Variational Transition States Calculated Using the Microcanonical Variational Transition State Theory

parameters	H−HCCCH (C_s-^2A'')		H_2CCC-H (C_s-^2A')	$H-H_2CCC$ (C_s-^2A')		$(C_2H_2)-CH$ (C_1-^2A)[e]		H−c-C_3H_2 (C_s-^2A')
R_C	2.3 [a]	2.4 [b]	2.2	1.9 [c]	2.0 [d]	2.3 [a]	2.5 [f]	2.0
ν_i	281.0	256.6	297.7	245.4	198.3	194.9	156.3	459.9
	318.8	292.5	316.7	291.8	288.6	230.0	178.9	535.1
	376.5	352.5	367.1	653.8	537.4	665.3	660.2	789.5
	417.2	417.7	485.1	741.4	616.5	673.4	668.8	900.5
	501.7	455.2	990.2	989.5	994.9	767.0	707.6	916.1
	515.8	480.6	1044.9	1052.3	1052.0	768.2	771.3	984.7
	701.0	638.7	1147.1	1062.9	1079.8	839.6	773.4	1085.0
	1232.9	1242.4	1481.3	1472.9	1475.6	2005.3	2030.5	1282.8
	1807.1	1783.1	2000.3	1927.5	1973.5	2810.0	2808.1	1645.2
	3352.4	3364.0	3103.4	3097.8	3095.8	3416.5	3419.3	3233.0
	3457.2	3456.2	3183.5	3181.0	3177.3	3510.4	3517.2	3269.6
E	−65.5	−63.2	−56.7	−55.1	−53.9	−51.5	−49.2	−69.5

[a] Corresponds to the $C(^3P) + C_2H_3$ reaction and photodissociation of propargyl radical at 193 nm. [b] Corresponds to the $HC(^2\Pi) + C_2H_2$ reaction and photodissociation of propargyl radical at 242 nm. [c] Corresponds to the $C(^3P) + C_2H_3$ reaction and photodissociation of propargyl radical at 193 and 242 nm. [d] Corresponds to the $HC(^2\Pi) + C_2H_2$ reaction. [e] Distance from the carbon atom of CH to the C≡C bond of acetylene. [f] Corresponds to photodissociation of propargyl radical at 242 nm.

TABLE 2: Calculated Microcanonical Rate Constants (in s^{-1}) for the $C(^3P) + C_2H_3(^2A')$ Reaction at a Collision Energy of 0.0 kcal/mol

rate constants	saddle-point method	Whitten−Rabinovitch's method
k_{1a}	3.21×10^{11}	3.21×10^{11}
k_{-1a}	3.98×10^{13}	3.98×10^{13}
k_{2a}	2.43×10^{11}	2.43×10^{11}
k_{-2a}	3.05×10^{12}	3.05×10^{12}
k_{3a}	3.90×10^{10}	3.90×10^{10}
k_{-3a}	2.88×10^{12}	2.88×10^{12}
k_{4a}	2.66×10^{11}	2.66×10^{11}
k_{-4a}	6.00×10^{11}	5.99×10^{11}
k_{5a}	2.90×10^{12}	2.89×10^{12}
k_{-5a}	6.61×10^{11}	6.60×10^{11}
k_{6a}	7.86×10^{11}	7.85×10^{11}
k_{-6a}	1.06×10^{12}	1.06×10^{12}
k_{7a}	9.94×10^{10}	9.92×10^{10}
k_{-7a}	2.00×10^{11}	1.99×10^{11}
k_{8a}	4.35×10^{12}	4.35×10^{12}
k_{-8a}	8.83×10^{11}	8.82×10^{11}
k_{9a}	9.36×10^{12}	9.35×10^{12}
k_{-9a}	9.46×10^{11}	9.46×10^{11}
k_{10a}	1.60×10^{10}	1.59×10^{10}
k_{11a}	7.30×10^{11}	7.29×10^{11}
k_{12a}	4.80×10^{10}	4.80×10^{10}
k_{13a}	8.56×10^{11}	8.56×10^{11}
k_{14a}	4.49×10^{11}	4.49×10^{11}
k_{15a}	1.90×10^{12}	1.90×10^{12}
k_{16a}	1.27×10^{11}	1.27×10^{11}
k_{17a}	7.43×10^{10}	7.42×10^{10}
k_{18a}	1.56×10^{11}	1.56×10^{11}
k_{19a}	4.48×10^{11}	4.47×10^{11}

TABLE 3: Calculated Microcanonical Rate Constants (in s^{-1}) for the $HC(^2\Pi) + C_2H_2(^1\Sigma_g^+)$ Reaction at a Collision Energy of 0.0 kcal/mol.

rate constants	saddle-point method	Whitten−Rabinovitch's method
k_{1b}	6.51×10^{10}	6.50×10^{10}
k_{-1b}	2.41×10^{13}	2.41×10^{13}
k_{2b}	5.63×10^{10}	5.62×10^{10}
k_{-2b}	3.06×10^{12}	3.06×10^{12}
k_{3b}	2.66×10^{8}	2.63×10^{8}
k_{-3b}	6.54×10^{11}	6.49×10^{11}
k_{4b}	2.45×10^{9}	2.41×10^{9}
k_{-4b}	7.47×10^{9}	7.34×10^{9}
k_{5b}	4.62×10^{11}	4.61×10^{11}
k_{-5b}	2.07×10^{11}	2.06×10^{11}
k_{6b}	2.39×10^{10}	2.37×10^{10}
k_{-6b}	4.85×10^{11}	4.81×10^{11}
k_{7b}	2.26×10^{9}	2.22×10^{9}
k_{-7b}	4.40×10^{9}	4.32×10^{9}
k_{8b}	3.64×10^{11}	3.62×10^{11}
k_{-8b}	1.04×10^{11}	1.04×10^{11}
k_{9b}	5.25×10^{12}	5.24×10^{12}
k_{-9b}	7.70×10^{11}	7.69×10^{11}
k_{10b}	1.69×10^{7}	1.68×10^{7}
k_{11b}	2.31×10^{9}	2.31×10^{9}
k_{12b}	4.96×10^{7}	4.96×10^{7}
k_{13b}	2.38×10^{10}	2.36×10^{10}
k_{14b}	9.63×10^{8}	9.57×10^{8}
k_{15b}	1.07×10^{10}	1.05×10^{10}
k_{16b}	8.08×10^{7}	8.12×10^{7}

are presented in Figures 2 and 3, respectively. The reaction scheme and branching ratios for photodissociation of propargyl radical are shown in Figure 4. Potential energy curves along the reaction coordinate for the $H_2C-C\equiv CH \rightarrow HCCCH(^3B) + H$ and $H_2C-C\equiv CH \rightarrow H_2CCC(^1A_1) + H$ channels are depicted in Figure 5. Finally, plots of concentrations versus time for various species in the $C(^3P) + C_2H_3$ and $CH(^2\Pi) + C_2H_2$ reactions and photodissociation of $H_2C-C\equiv CH$ at 242 nm are shown in panels a, b, and c, respectively, of Figure 6.

4. Discussion

4.1. $C(^3P) + C_2H_3(^2A')$ Reaction. As seen in Figure 2, there are two possibilities for an addition of $C(^3P)$ to the $C_2H_3(^2A')$ radical. $C(^3P)$ can add either to the carbon atom with an unpaired electron to form isomer **5** or to the C═C bond to give isomer **4**. Product branching ratios depend on a branching ratio of these two channels at the initial reaction stage. To determine this branching ratio, dynamics calculations using analytical PES would be required, which is beyond the scope of this paper. Here, we varied initial concentrations of isomers **4** and **5** while their total concentration was fixed at 100. The product branching ratios calculated with various initial concentrations of isomers **4** and **5** are shown in Table 5. As seen in Table 5, when the initial concentration of isomer **5** decreases and that of isomer **4** increases, the amount $H_2CCC + H$ products decreases, but those of $HCCCH(^3B) + H$ of and c-$C_3H_2 + H$ increase, while the amounts of $HCCC(^2A') + H_2$ and $CH(^2A') + C_2H_2$ remain nearly constant. However, the margins of all the changes are narrow and do not exceed 1.2%, 3.5%, and ~3.7% for c-$C_3H_2 + H$, $HCCCH(^3B) + H$, and $H_2CCC + H$, respectively. The results show that the $C_3H_2 + H$ products dominate the reaction contributing about 93%. Therefore, the $C(^3P) + C_2H_3(^2A')$ reaction is expected to produce mostly the C_3H_2 isomers and

TABLE 4: Calculated Microcanonical Rate Constants (in s^{-1}) for the Photodissociation of Propargyl Radical $H_2C-C\equiv CH(C_{2v}-{}^2B_1)$ at 193 and 242 nm

rate constants	193 nm (148.17 kcal/mol) [a]	242 nm (118.17 kcal/mol) [a]
k_{1c}	2.91×10^{11}	1.04×10^{11}
k_{-1c}	3.87×10^{13}	2.81×10^{13}
k_{2c}	2.22×10^{11}	8.60×10^{10}
k_{-2c}	3.05×10^{12}	3.06×10^{12}
k_{3c}	3.00×10^{10}	1.39×10^{9}
k_{-3c}	2.70×10^{12}	1.14×10^{12}
k_{4c}	2.11×10^{11}	1.24×10^{10}
k_{-4c}	4.86×10^{11}	3.47×10^{10}
k_{5c}	2.61×10^{12}	8.17×10^{11}
k_{-5c}	6.20×10^{11}	2.99×10^{11}
k_{6c}	6.56×10^{11}	7.62×10^{10}
k_{-6c}	1.02×10^{12}	6.45×10^{11}
k_{7c}	8.24×10^{10}	8.28×10^{9}
k_{-7c}	1.65×10^{11}	1.63×10^{10}
k_{8c}	3.81×10^{12}	8.17×10^{11}
k_{-8c}	7.90×10^{11}	2.11×10^{11}
k_{9c}	9.05×10^{12}	6.25×10^{12}
k_{-9c}	9.35×10^{11}	8.21×10^{11}
k_{10c}	1.15×10^{10}	1.94×10^{8}
k_{11c}	5.52×10^{11}	1.74×10^{10}
k_{12c}	3.46×10^{10}	5.75×10^{8}
k_{13c}	7.11×10^{11}	7.80×10^{10}
k_{14c}	3.44×10^{11}	1.03×10^{10}
k_{15c}	1.49×10^{12}	6.91×10^{10}
k_{16c}	9.49×10^{10}	1.63×10^{9}
k_{17c}	4.89×10^{10}	7.01×10^{7}
k_{18c}	1.10×10^{11}	1.49×10^{8}
k_{19c}	3.28×10^{11}	3.85×10^{9}

[a] Calculated using the saddle-point method.

TABLE 5: Calculated Product Branching Ratios (in %) for the $C(^3P) + C_2H_3(^2A')$ Reaction at Various Initial Concentrations of Isomers 4 and 5

isomer **4**	isomer **5**	c-C_3H_2 + H	H + HCCCH(^{3}B)	H + H_2CCC	H_2 + HCCC	HC($^2\Pi$) + C_2H_2
0	100	6.1	78.3	8.1	5.5	2.0
10	90	6.3	78.6	7.7	5.5	1.9
20	80	6.4	79.0	7.3	5.5	1.8
30	70	6.5	79.3	7.0	5.5	1.7
40	60	6.6	79.7	6.6	5.5	1.6
50	50	6.7	80.0	6.3	5.5	1.5
60	40	6.8	80.4	5.9	5.5	1.4
70	30	7.0	80.7	5.5	5.5	1.3
80	20	7.1	81.1	5.1	5.5	1.2
90	10	7.2	81.4	4.8	5.5	1.1
100	0	7.3	81.8	4.4	5.5	1.0

TABLE 6: Calculated Product Branching Ratios (in %) for the $HC(^2\Pi) + C_2H_2(^1\Sigma_g+)$ Reaction at Various Initial Concentrations of Isomers 2 and 6

isomer **2**	isomer **6**	c-C_3H_2 + H	H_2 + HCCC	HCCCH(^{3}B) + H	H + H_2CCC
0	100	10.2	1.9	87.0	0.9
10	90	10.4	1.9	86.8	0.9
20	80	10.7	1.9	86.5	0.9
30	70	11.0	1.9	86.2	0.9
40	60	11.2	1.9	86.0	0.9
50	50	11.5	1.8	85.8	0.9
60	40	11.8	1.8	85.5	0.9
70	30	12.0	1.8	85.3	0.9
80	20	12.3	1.8	85.0	0.9
90	10	12.6	1.8	84.7	0.9
100	0	12.8	1.8	84.5	0.9

only a minor amount (5.5%) of HCCC + H_2. It should be mentioned that a careful investigation of PES[10] did not show any pathway for molecular hydrogen elimination from cyclic intermediates **2** and **4**, so the cyclic c-C_3H isomer is not likely to be produced. Interestingly, the CH($^2\Pi$) + C_2H_2 branching ratio is 1−2%, so a trace amount of these products can be also formed. We would like to stress that the CH product is not formed in a direct reaction via an H atom abstraction by the carbon atom but through decomposition of a bound intermediate. The most interesting result, however, is the largest branching ratio of HCCCH(^{3}B) among the C_3H_2 isomers. The propargyl radical (isomer **1**) is the key intermediate of the $C(^3P) + C_2H_3$-($^2A'$) reaction; its formation is very fast (see Figure 6a) from both initial intermediates **5** ($k_{-2a} = 3.05 \times 10^{12}$ s^{-1}) and **4** ($k_{-1a} = 3.98 \times 10^{13}$ s^{-1}). Isomer **1** can decompose to HCCCH(^{3}B) + H and H_2CCC + H or isomerize to the cyclic isomer **2** by two pathways, **1** → **6** → **2** and **1** → **4** → **2**, which, in turn, dissociate to c-C_3H_2 + H. The rate constant for the **2** → c-C_3H_2 + H dissociation is high ($k_{13a} = 8.56 \times 10^{11}$ s^{-1}); however, the rates for the critical isomerization steps **1** → **6** and **4** → **2** ($k_{3a} = 3.90 \times 10^{10}$ and $k_{-4a} = 6.00 \times 10^{11}$ s^{-1}, respectively) are slower than the rate for the **1** → HCCCH(^{3}B) + H decomposition ($k_{11a} = 7.30 \times 10^{11}$ s^{-1}). Although the transition states for the **1** → **6** and **4** → **2** steps lie lower in energy than HCCCH(^{3}B) + H, these transition states correspond to hydrogen migrations and have much tighter geometries than the loose variational TS for the **1** → HCCCH(^{3}B) + H barrierless dissociation. The tighter structures lead to the smaller total numbers of states $W^{\neq}$ resulting in lower rate constants. As a final outcome, the calculated HCCCH(^{3}B) + H branching ratio is a factor of 11−13 higher than that of c-C_3H_2 + H.

Although the energy difference between HCCCH(^{3}B) and H_2-CCC($^1A_1$) is only 1 kcal/mol, the corresponding rate constants for the dissociation of isomer **1**, k_{11a} and k_{10a}, differ by 45.7 times. This can be attributed to the different behavior of the HCCCH(^{3}B) + H and $H_2CCC(^1A_1)$ + H potential energy curves along the reaction coordinate when hydrogen atom approaches C_3H_2 (see Figure 5). $H_2CCC(^1A_1)$ + H is a reaction of a closed shell singlet species with a radical, which might have a barrier (it does not for the $H_2CCC(^1A_1)$ + H → **1** case), and the potential curve is much less attractive than the potential energy curve for HCCCH(^{3}B) + H, the reaction of two radical species. As a result, the variational TS for the former occurs at significantly higher energy than for the latter and possesses much lower total number of states slowing down the corresponding rate constant k_{10a}. Therefore, the $H_2CCC(^1A_1)$ + H products contribute only 4−8%. It should be noted that we carried out the variational TS search for the triplet HCCCH + H channel within C_s symmetry and ^{2}A" electronic state, correlating to the HCCCH(C_s, ^{3}A") products. However, the $C_s(^3A")$ and $C_2(^3B)$ structures of HCCCH are nearly degenerate with the former lying only 0.16 and 0.20 kcal/mol higher than the latter at the CASPT2[34] and CCSD(T)[35] levels, respectively.

The transition state for H_2 elimination from **1** also lies slightly lower than the products of the hydrogen atom splitting, HCCCH-(^{3}B) and $H_2CCC(^1A_1)$. However, this transition state is tighter than those for atomic hydrogen lost, and rate constant k_{12a} for the **1** → HCCC + H_2 reaction step is ∼40 times lower than k_{11a}, rendering the H_2 loss only a minor (∼5%) channel.

Since all C_3H_2 isomers are formed essentially without exit barriers, the calculated branching ratios may be sensitive to the energy differences between them. In turn, the energy gap between c-C_3H_2 and HCCCH(^{3}B) decreases from the 12.5 kcal/mol obtained by us[10] at the RCCSD(T)/6-311+G(3df,2p) + ZPE level to 9.8 kcal/mol at CCSD(T)/cc-pVTZ[35] and 4.9 kcal/mol from the recent CASPT2 calculations.[34] This means that the HCCCH(^{3}B) + H branching ratio may be even higher than 78−

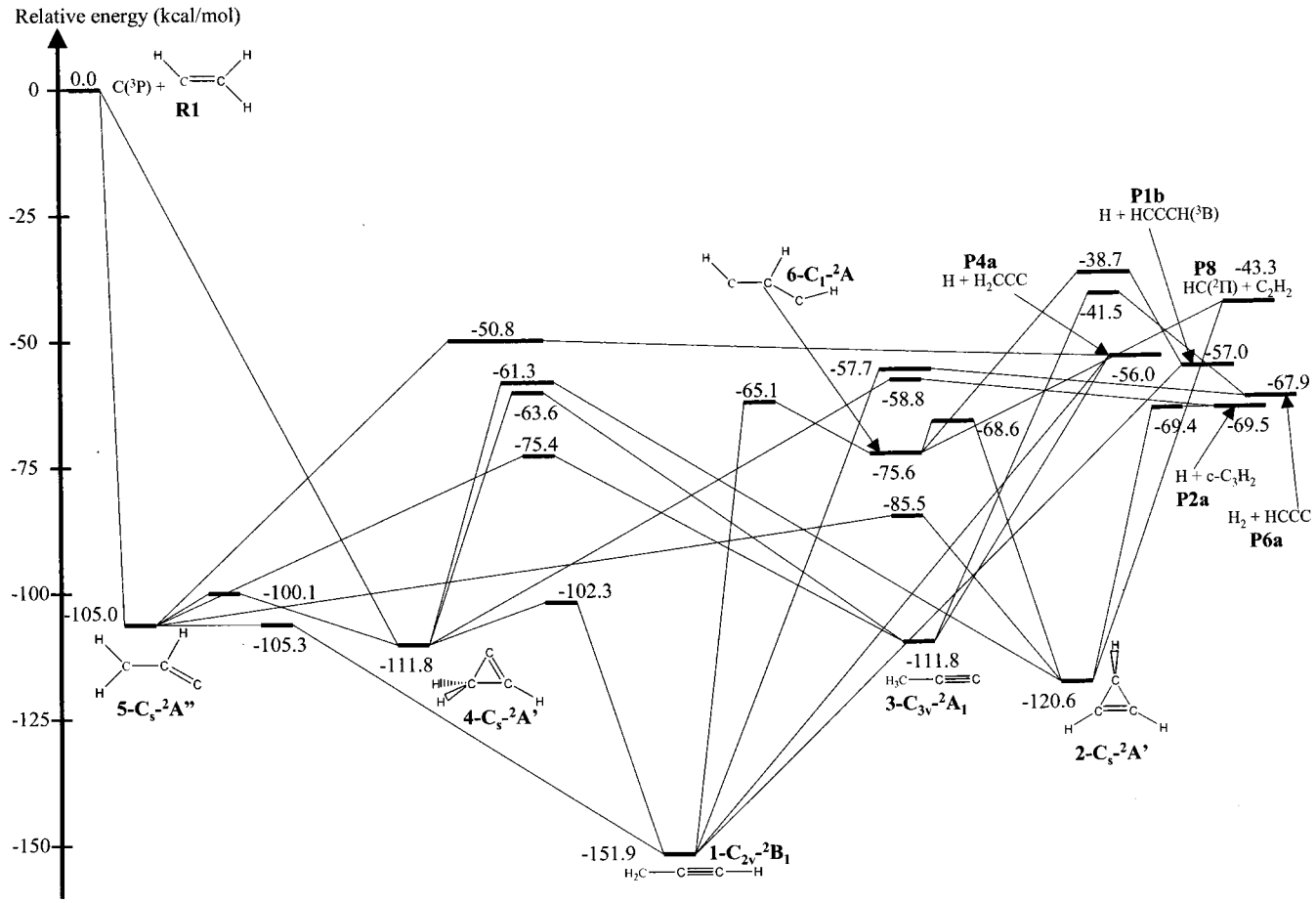

Figure 1. Potential energy diagram of the C_3H_3 system in the ground electronic state. The relative energies are calculated at the RCCSD(T)/6-311+G(3df,2p)//B3LYP/6-311G(d,p) + ZPE[B3LYP/6-311G(d,p)] level of theory. (Adapted from ref 10.)

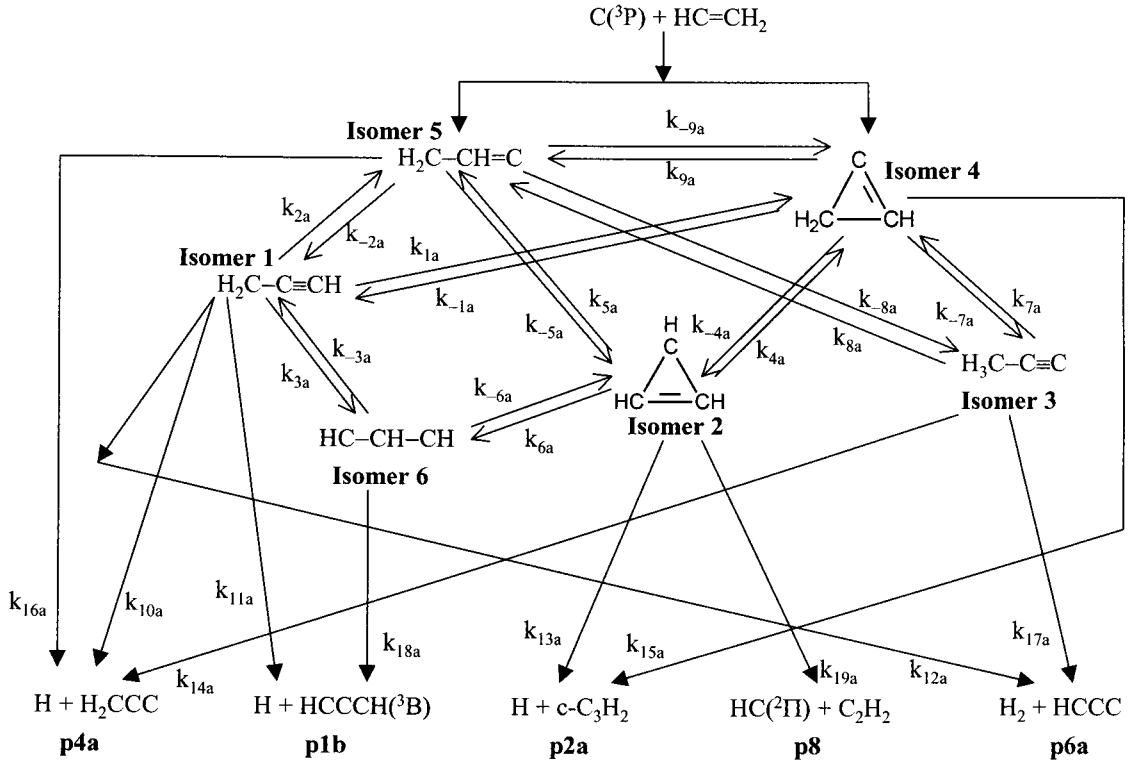

Figure 2. Reaction scheme used for kinetic calculations for the $C(^3P) + C_2H_3$ reaction.

82% obtained here. Finally, as we concluded earlier,[10] if the $C(^3P) + C_2H_3$ reaction occurs on the first excited state PES, the most probable product should be the electronically excited $HCCCH(^1A")$ isomer. The latter can eventually undergo inter-

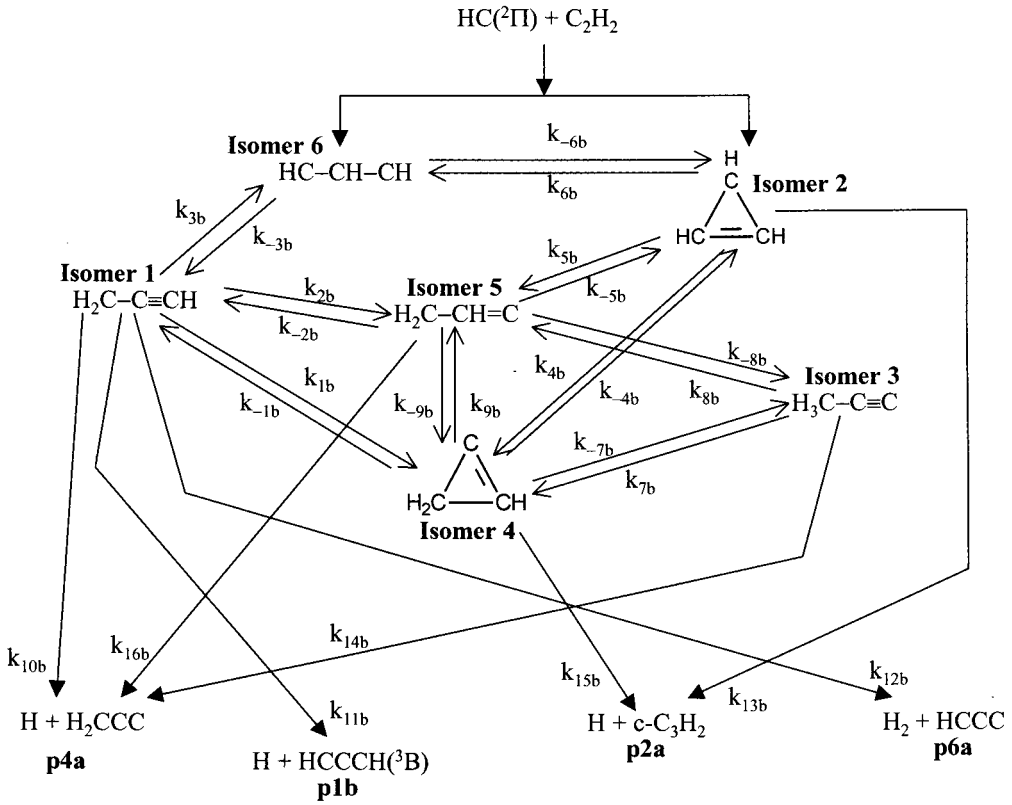

Figure 3. Reaction scheme used for kinetic calculations for the $CH(^2\Pi) + C_2H_2$ reaction.

system crossing to the ground triplet state in the low-density interstellar clouds prior to its reactions with other species.

4.2. $CH(^2\Pi) + C_2H_2$ Reaction. This reaction occurs on the same C_3H_3 PES and was theoretically investigated by Vereecken et al.,[23] whose RRKM calculations over extended temperature and pressure ranges showed that typical branching ratios are 82−90% and 7−11% for $HCCCH(^3B)$ and c-C_3H_2, respectively. As seen in Figure 3, there are two possibilities for the addition of $CH(^2\Pi)$ to the $C_2H_2(^1\Sigma_g^+)$ molecule. $CH(^2\Pi)$ can add either to one of the carbon atoms to form isomer **6** or to the C≡C bond to give isomer **2**. In both cases, the additions do not have any entrance barrier. The product branching ratios slightly depend on the initial branching ratio of these two channels. As shown in Table 6, we carried out the calculations using various initial concentrations of isomers **2** and **6**. According to our results, the C_3H_2 products are dominant contributing ∼98% of the total amount of the reaction products, while $HCCC(^2A')$ and H_2 give only ∼2%. The contribution of the H_2CCC isomer is also minor, 0.9%. The major products are $HCCCH(^3B) + H$ (84.5−87%) and c-C_3H_2 + H (12.8−10.2%). Thus, the product distribution in the $CH(^2\Pi) + C_2H_2$ reaction is quite similar to that for $C(^3P) + C_2H_3$ but the amount of the c-C_3H_2 + H products increases. This can be attributed to the fact that for the CH + C_2H_2 reaction the cyclic C_3H_3 isomer **2** is one of the initial intermediates. This is seen in Figure 6b; isomer **1** appears in parallel with disappearance of **2** and the $HCCCH(^3B)$ + H products start to form later than c-C_3H_2 + H, only when the concentration of **1** becomes significant. Product **2** can be formed directly from the reactants or from another initial intermediate **6** via a low barrier, $k_{-6b}(\mathbf{6} \rightarrow \mathbf{2}) = 4.85 \times 10^{11}\ s^{-1}$. Once isomer **2** is produced, the rate constants for its decomposition to c-C_3H_2 ($k_{13b} = 2.38 \times 10^{10}\ s^{-1}$) is about 1 order of magnitude lower than that for the **2** → **5** isomerization ($k_{5b} = 4.62 \times 10^{11}\ s^{-1}$) eventually leading to isomer **1**, but still some fraction of c-C_3H_2 can be produced. When the initial concentration of **6** increases, some portion of molecules undergoes the **6** → **1** isomerization ($k_{-3b}/k_{-6b} = 1.35$) instead of producing **2**. This results in the increase of the $HCCCH(^3B)$ + H branching ratio from 84.5% to 87% and corresponding decrease of the branching ratio for c-C_3H_2 + H (Table 6). In any case, the $CH(^2\Pi) + C_2H_2$ reaction is expected to be a somewhat better source of the cyclic C_3H_2 isomer than $C(^3P) + C_2H_3$, although c-C_3H_2 remains only the second important product.

The product branching ratios calculated here for the collision-free conditions are similar to those reported by Vereecken and Peeters[23b] for the temperatures up to 2000 K and pressures up to several atmospheres. It should be noted that Vereecken and Peeters suggested three possible initial intermediates in the $CH(^2\Pi) + C_2H_2$ reaction, **2** (after cycloaddition of CH to acetylene), **6** (after chain addition), and **1** (after direct insertion of CH into a C−H bond). Although the direct insertion would bring the largest energy gain, the large entropy change associated with it would slow this channel so that it would be unlikely to compete with the two-step process (chain addition followed by a 1,2-H shift). To address a feasibility and competitiveness of the three channels dynamics calculations would be necessary. Meanwhile, due to high isomerization rates, the relative product yields are not very sensitive to the initial branching. For example, at 1500 K and 1 atm, the HCCCH/c-C_3H_2 ratio was calculated as 75/15, 82/9, and 91/2 for 100% cycloaddition, chain addition, and insertion, respectively.[23b] If we add the possibility of the insertion in our calculations, the yield of $HCCCH(^3B)$ may increase to ∼90% and that of c-C_3H_2 may decrease to ∼5%. This can be derived from our results for photodissociation of $H_2CC{\equiv}CH$ (**1**) at 242 nm, where the available internal energy of intermediate **1** is quite similar to that it acquires from chemical activation in the $CH(^2\Pi) + C_2H_2$ reaction. Therefore, the photodissociation process (assuming fast internal conversion) can be considered as an approximate model of the $CH(^2\Pi) + C_2H_2$ reaction proceeding exclusively by insertion to form **1**.

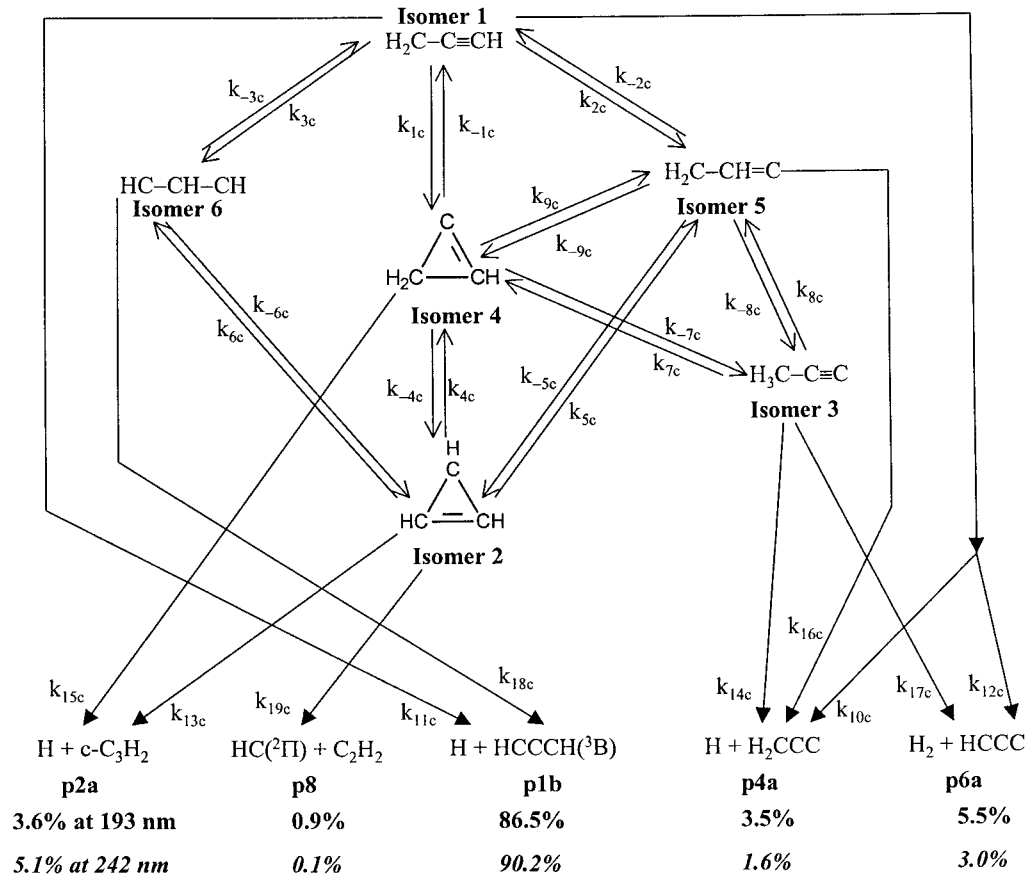

Figure 4. Reaction scheme used for kinetic calculations of photodissociation of the propargyl radical at 193 and 242 nm. The numbers in the bottom show calculated product branching ratios.

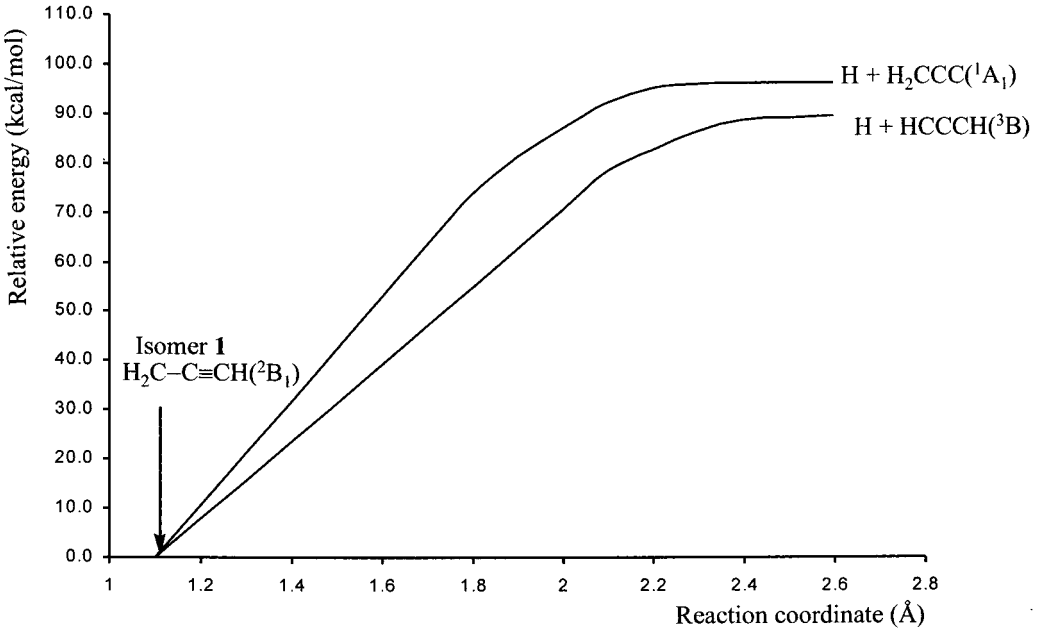

Figure 5. Potential energy curves along the reaction coordinate for the $H_2C-C\equiv CH \rightarrow HCCCH(^3B) + H$ and $H_2C-C\equiv CH \rightarrow H_2CCC(^1A_1) + H$ channels calculated using the RCCSD(T)/6-311+G(3df,2p) method.

4.3. Photodissociation of $H_2C-C\equiv CH$ at 193 nm. The propargyl radical ($H_2C-C\equiv CH$, C_{2v}, $^2B_1$), a primary product of the reaction of atomic carbon with ethylene[36] and of allene photodissociation at 193 nm, can absorb a second 193 nm photon and decompose.[25] On the basis of the molecular beam studies of secondary photodissociation of the propargyl radical, Jackson, Lee, and co-workers suggested relative branching ratios as 96% for the $C_3H_3 \rightarrow C_3H_2 + H$ channel and 4% for the $C_3H_3 \rightarrow C_3H + H_2$ channel. We assume that the photon energy of 193 nm is used to produce the vibrationally excited propargyl radical, which then can isomerize and undergo atomic and molecular hydrogen elimination processes, leading to various

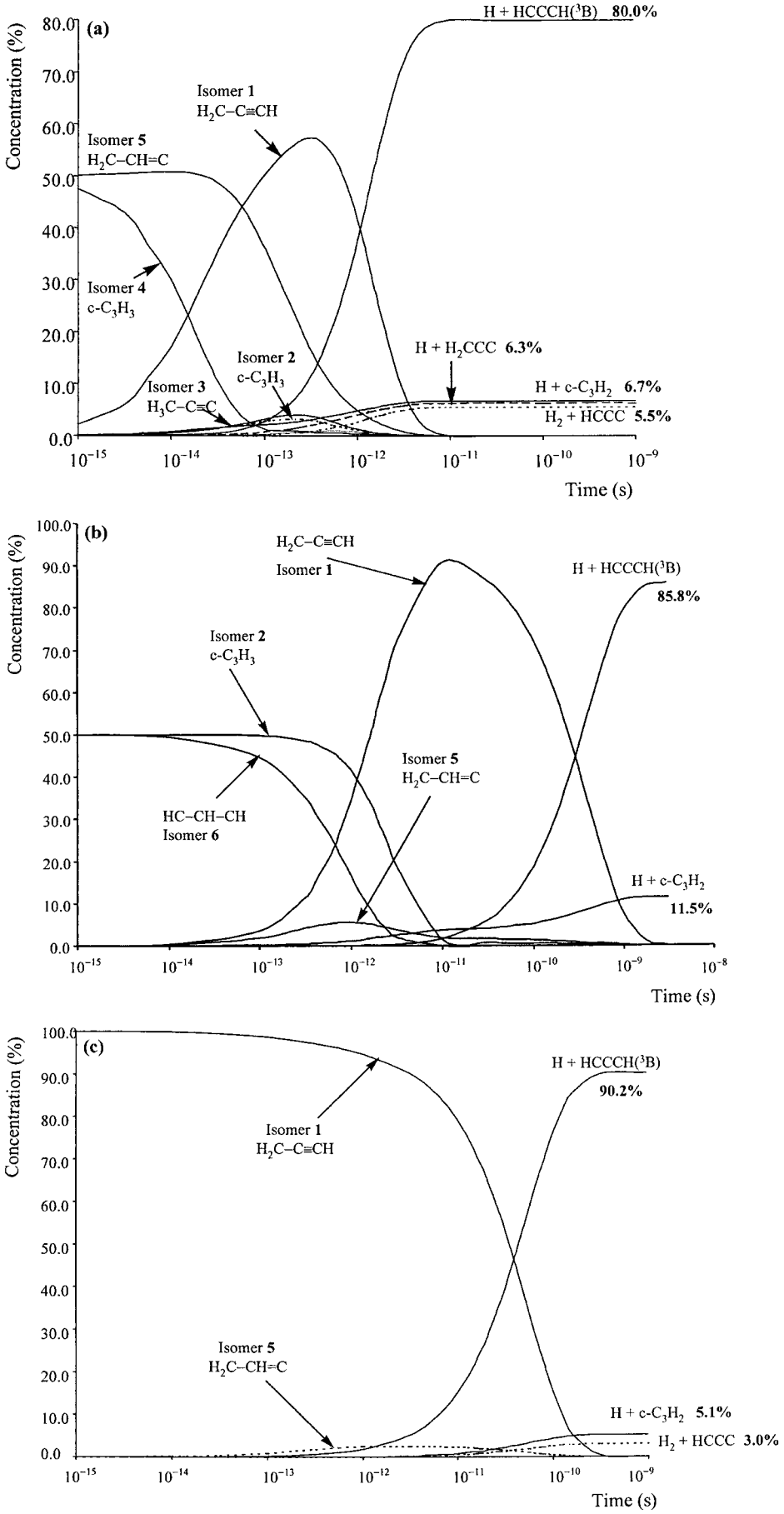

Figure 6. Concentrations of various intermediates and products versus time. (a) The $C(^3P) + C_2H_3(^2A')$ reaction (initial concentration ratio of isomers **4** and **5** is taken as 50/50). (b) The $CH(^2\Pi) + C_2H_2(^1\Sigma_g^+)$ reaction (initial concentration ratio of isomers **2** and **6** is taken as 50/50). (c) Photodissociation of propargyl radical at 242 nm.

products as presented in Figure 4. The calculated branching ratios are also shown in Figure 4, while microcanonical rate constants are collected in Table 4.

As seen in Figure 4, the branching ratios are 86.5% for the $HCCCH(^3B) + H$ products, 3.6% for $c\text{-}C_3H_2 + H$, 5.5% for $HCCC(^2A') + H_2$, 3.5% for $H_2CCC + H$, and 0.9% for the $CH(^2\Pi) + C_2H_2$ products. Thus, the $HCCCH(^3B) + H$ product channel is the most important, followed by the $HCCC(^2A') + H_2$ channel. Some comparisons with the experimental results[25] can be made. According to the calculations, the $CH(^2\Pi) + C_2H_2$ channel gives a small contribution of 0.9% and was obtained in experiment in trace amounts. Our evaluated $[C_3H_2 + H]$:$[C_3H + H_2]$ ratio is 93.6:5.5, in good agreement with 96:4 obtained in experiment.[25] Evidently, the molecular hydrogen elimination channel is much less probable than the atomic hydrogen elimination channel.

As compared to the $C(^3P) + C_2H_3$ reaction, the branching ratio of the $HCCCH(^3B) + H$ products increases by 5−8%, and that of $c\text{-}C_3H_2 + H$ decreases. In the two processes the propargyl radical (isomer **1**) possesses, similar amounts of energy (151.9 kcal/mol in the reaction and 148.2 kcal/mol in photodissociation after internal conversion into vibrationally excited ground electronic state). However, we assumed here that the dissociation process after photoexcitation and internal conversion starts from the energized isomer **1**, which prefers to decompose to $HCCCH(^3B) + H$. On the other hand, in the $C(^3P) + C_2H_3$ reaction isomers **4** and **5** are formed first and isomer **1** can be bypassed by the **5** → **2** and **4** → **2** rearrangements enhancing the production of $c\text{-}C_3H_2$. Interestingly, the branching ratio of $H_2CCC + H$ in the reaction is also slightly higher than that in photodissociation, apparently due to the possibility of the **5** → **3** and **4** → **3** isomerizations followed by the atomic hydrogen elimination from H_3CCC (isomer **3**). The resulting branching ratios for the photodissociation process would depend on what happens with the molecule in the excited electronic state upon photoexcitation. For instance, if the system has enough time to isomerize to some other configuration before internal conversion, this would change initial concentration of vibrationally hot C_3H_3 isomers leading to different product branching ratios.

4.4. Photodissociation of $H_2C-C\equiv CH$ at 242 nm. The reaction scheme and calculated branching ratios for photodissociation of the propargyl radical at 242 nm are shown in Figure 4, while the microcanonical rate constants are presented in Table 4. The results are rather similar to those obtained for the $CH(^2\Pi) + C_2H_2$ reaction; the branching ratios are 90.2% for the $HCCCH(^3B) + H$ channel, 5.1% for $c\text{-}C_3H_2 + H$, 3.0% for $HCCC(^2A') + H_2$, 1.6% for $H_2CCC + H$, and 0.1% for the $CH(^2\Pi) + C_2H_2$ products. On the basis of their experimental measurements of photodissociation dynamics of the propargyl radical at 240−265 nm, Deyerl et al.[26] suggested that $c\text{-}C_3H_2$ and H are the dominant reaction products. This suggestion was supported by experimental translational energy release, which is in agreement with a reaction proceeding via a barrier of around 90 kcal/mol. Our RCCSD(T)/6-311+G(3df,2p) calculations[10] gave the reaction energies as 82.4 and 94.9 kcal/mol for the $c\text{-}C_3H_2 + H$ and $HCCCH(^3B) + H$ product channels, respectively. Therefore, the measured transitional energy distribution consistent with a 90 kcal/mol barrier may be due to a convolution of signals from the $c\text{-}C_3H_2$ and $HCCCH(^3B)$ isomers.

Deyerl et al.[26] also observed isotope scrambling during photodissociation of the $H_2C-C\equiv CD$ radical. The analysis of PES and calculated rate constants shows that isotope scrambling may precede the dissociation by the following mechanisms: **1** → **5** → **2** → **5** → **1** and **1** → **5** → **3** → **5** → **1**. The barriers for all the steps involved in these rearrangements are at least 6 kcal/mol lower than the barriers for dissociation of either **1** to $HCCCH(^3B) + H$ or **2** to $c\text{-}C_3H_2 + H$. The slowest rate along these pathways, k_{2c}(**1** → **5**), is ∼5 times faster than k_{11c}(**1** → $HCCCH(^3B) + H$), so the system would have enough time for isotope scrambling before it dissociates. The **1** → **5** → **2** isomerization can result in the $c\text{-}C_3H_2 + H$ products; however, since k_{13c}(**2** → $c\text{-}C_3H_2 + H$) is ∼73% lower than k_{5c}(**2** → **5**), a substantial fraction of molecules would isomerize back to isomer **5**. The **1** → **5** → **3** → **5** → **1** rearrangement would dominantly lead to isotope scrambling because the dissociation rate of **3** (k_{14c}) is slow. Rate constants k_{-5c}(**5** → **2**) and k_{-8c}(**5** → **3**) are comparable; therefore, the two mechanisms of isotope scrambling can compete and another one, **1** → **4** → **3** → **4** → **1**, may also contribute.

The available experimental evidence[26] which includes observations of the translational energy distribution and isotope scrambling does not appear to be sufficient to unambiguously conclude that the $c\text{-}C_3H_2 + H$ channel is dominant. The use of spectroscopic methods, which can clearly distinguish between $HCCCH(^3B)$ and $c\text{-}C_3H_2$, to monitor the product formation could be one of the ways to determine the branching ratios more definitely.

The calculated microcanonical rate constants (Table 4) are significantly higher than the rate for the formation of H atoms reported by Deyerl et al.,[26] 1.3×10^7 s^{-1}. If we adjust the reaction energy for the formation of $c\text{-}C_3H_2$ to 90 kcal/mol and scale the frequencies of isomer **1** by a factor of 0.71 to take into account anharmonicity (as was done by Deyerl et al.), the calculated rates can be lowered by 2−3 orders magnitude to the 10^7-10^8 s^{-1} range. It should be mentioned that the energies of the **1** → $c\text{-}C_3H_2 + H$ and **1** → $HCCCH(^3B) + H$ reactions may have certain error bars. For instance, these energies are 82.4 and 94.9 kcal/mol, respectively, at the RCCSD(T)/6-311+G(3df,2p) + ZPE level, but increase to 86.2 and 99.4 kcal/mol if we use the heats of formation $\Delta H_f^\circ{}_0$ of the involved species evaluated by us earlier on the basis of calculations of heats of isodesmic reactions at the CCSD(T) and G3 levels.[10] Meanwhile, such an energy change affects the rate constants only moderately, by 2−3 times. The largest decrease of the rates (by ∼2 orders of magnitude) can be achieved by scaling the frequencies. However, anharmonicity has to be taken into account in a more appropriate way, and a more sophisticated RRKM treatment is required to obtain more accurate absolute values of microcanonical rate constants.

5. Conclusions

The $C(^3P) + C_2H_3(^2A')$ and $CH(^2\Pi) + C_2H_2$ reactions were studied to investigate possible formations of C_3H_2 and C_3H isomers in extraterrestrial environments, combustion processes, and CVD. Microcanonical rate constants were calculated using RRKM theory based on harmonic frequencies computed at the B3LYP/6-311G(d,p) level. The fourth-order Runge−Kutta method was utilized to solve the system of kinetic equations. Numerical solutions obtained give concentrations of intermediates and products as functions of time and the converged concentrations were used for calculations of product branching ratios. Product branching ratios for the $C(^3P) + C_2H_3(^2A')$ reaction are obtained as 78.3−81.8% for the $HCCCH(^3B) + H$ products, 6.1−7.3% for $c\text{-}C_3H_2 + H$, 4.4−8.1% for $H_2CCC + H$, 5.5% for $HCCC + H_2$, and 1−2% for the $CH(^2\Pi) + C_2H_2$ products, depending on the initial concentrations of intermediates **4** and **5**, both of which can be produced at the initial reaction

step without entrance barrier. Therefore, the $C(^3P) + C_2H_3(^2A')$ reaction can be expected to mostly produce C_3H_2 isomers in extraterrestrial environments. Product branching ratios for the $CH(^2\Pi) + C_2H_2$ reaction vary with the initial concentrations of intermediates **2** and **6**, which can be formed from the reactants without barriers and are calculated as 84.5−87% for HCCCH-(^{3}B) + H, 10.2−12.8% for c-C_3H_2 + H, ∼2% for HCCC + H_2, and 0.9% for H_2CCC + H. The product branching ratios are slightly different from those for the $C(^3P) + C_2H_3(^2A')$ reaction, indicating that the $CH(^2\Pi) + C_2H_2$ reaction should be a better source of the cyclic C_3H_2 isomer than the $C(^3P) + C_2H_3(^2A')$ reaction, although c-C_3H_2 remains only the second most important product. The product branching ratios computed for $CH(^2\Pi) + C_2H_2$ reaction under collision-free conditions are similar to those obtained Vereecken and Peeters[23b] for a wide range of temperatures and pressures.

The photodissociation of propargyl radical was also investigated at photon energies of 193 and 242 nm. Product branching ratios calculated at 193 nm are 86.5% for the HCCCH(^{3}B) + H channel, 3.6% for c-C_3H_2 + H, 5.5% for HCCC($^2A'$) + H_2, 3.5% for H_2CCC + H, and 0.9% for $CH(^2\Pi) + C_2H_2$. The calculated [C_3H_2+H]/[C_3H+H] branching ratio of 93.6:5.5 closely agrees with the experimental value of 96:4.[25] Product branching ratios obtained at 242 nm are 90.2% for HCCCH-(^{3}B) + H, 5.1% for c-C_3H_2 + H, 3.0% for HCCC($^2\Pi$) + H_2, 1.6% for H_2CCC + H, and 0.1% for $CH(^2\Pi) + C_2H_2$. Thus, HCCCH(^{3}B) and H are predicted to be the major products, followed by c-C_3H_2 + H. Further experimental studies are suggested in order to quantify the branching ratios of various C_3H_2 isomers, for instance, product formation monitoring using spectroscopic methods which can distinguish between HCCCH-(^{3}B) and c-C_3H_2. It should be mentioned that in our calculations we did not consider the effect of angular momentum, which may be significant for the two heavy-fragment reactions, such as $C + C_2H_3$ and $CH + C_2H_2$, producing heavy + light product pairs. We intend to improve the RRKM treatment by taking into account the k(J,E) effects in our future studies.

Our investigations demonstrated explicitly that three C_3H_2 isomers can be formed via neutral−neutral reactions in the interstellar medium, i.e., c-C_3H_2, H_2CCC, and HCCCH. Surprisingly, although the present study predicts the latter to be an important product, it has never been observed astronomically. This might be likely due to the small dipole moment of 0.51 D compared to 3.35 D for c-C_3H_2 and 4.24 D for H_2CCC. Nevertheless, our study might fuel prospective searches of this hitherto undetected isomer (rotational constants are 4176.2, 10.2, and 10.2 GHz), especially toward cold molecular clouds TMC-1 and OMC-1 via microwave spectroscopy. HCCCH should be observable in the circumstellar envelope of IRC+10216 as well, but the higher temperatures close to the photosphere might complicate the pure rotational spectrum as the HCCCH molecule is very floppy, and the bending mode with the frequency of 105 cm^{-1} at the B3LYP/6-311G** level[10] (ca. with 170 and 132 cm^{-1} by the CASSCF[34] and CCSD(T)[37] methods and experimental value of 249 cm^{-1} measured[37] in argon matrix at 8 K) could be excited. On the other hand, this absorption could match hitherto unassigned infrared bands recorded within the framework of the ISO observations of IRC+10216.

Last but not least, our comprehensive study should lead to a reformation of current reaction networks modeling chemical reaction networks in cold molecular clouds and outflow of carbon stars. For the first time, it is feasible to include distinct C_3H_2 isomers into these networks. Second, the calculated branching ratios deviate strongly from predictions based on simple thermochemistry as, for example, HCCCH is the major reaction product of the C/C_2H_3 reaction but not the thermodynamically most stable c-C_3H_2 isomer. Most important, our studies suggest a hitherto not considered pathway to form interstellar CH radicals, i.e., the reaction of atomic carbon with the vinyl radical. The actual contribution of this pathway to the interstellar CH chemistry should be tackled in novel reaction networks. This underlines the importance to investigate the complete potential energy surfaces involved in important interstellar reactions rather guessing product distributions from simple thermochemistry.

Acknowledgment. This work was supported in part by Academia Sinica and National Science Council of Taiwan, R. O. C. under Grant NSC 90-2113-M-001-068 and by Chinese Petroleum Research Fund. T.L.N. is grateful to IAMS for a visiting fellowship. This work was performed within the International Astrophysics Network. We are thankful to Professor J. Peeters and Dr. L. Vereecken for their helpful comments concerning this work and beneficial discussions.

References and Notes

(1) Thaddeus, P.; Vrtilek, J. M.; Gottlieb, C. A. *Astrophys. J. Lett.* **1985**, *299*, 63.
(2) Matthews, H. E.; Irvine, W. M. *Astrophys. J. Lett.* **1985**, *298*, 61.
(3) Green, S. *Astrophys. J.* **1980**, *240*, 962.
(4) Turner, B. E. *Astrophys. J. Lett.* **1989**, *347*, L39.
(5) Kuiper, T. B.; Whiteoak, J. B.; Peng, R. S.; Peter III, W. L.; Reynolds, J. E. *Astrophys. J. Lett.* **1993**, *416*, 33.
(6) Turner, B. E.; Rickard, L. J.; Xu, L. P. *Astrophys. J.* **1989**, *344*, 292.
(7) Cernicharo, J. et al. *Astrophys. J. Lett* **1991**, *368*, 39.
(8) Kaiser, R. I.; Ochsenfeld, C.; Stranges, D.; Head-Gordon, M.; Lee, Y. T. *Faraday Discuss.* **1998**, *109*, 183.
(9) Madden, S. C. In *Chemistry in Space*; Greenberg, J. M., Pirronello, V., Eds.; Kluwer: Dordrecht, 1991; p 437 and references therein.
(10) Nguyen, T. L.; Mebel, A. M.; Kaiser, R. I. *J. Phys. Chem. A* **2001**, *105*, 3284.
(11) Wu, C.; Kern, R. *J. Chem. Phys.* **1987**, *91*, 6291.
(12) Alkemade, V.; Homann, K. *Z. Phys. Chem. Neue Folge* **1989**, *161*, 19.
(13) Kern, R. D.; Singh, H. J.; Wu, C. H. *Int. J. Chem. Kinet.* **1988**, *20*, 731.
(14) Westmoreland, P.; Dean, A.; Howard, J.; Longwell, J. *J. Chem. Phys.* **1989**, *93*, 8171.
(15) Hidaka, Y.; Nakamura, T.; Miyauchi, A.; Shiraishi, T.; Kawano, H. *Int. J. Chem. Kinet.* **1989**, *29*, 643.
(16) Stein, S.; Walker, J.; Suryan, M.; Farh, A. *23rd Symp. (Int.) Comb.* **1991**, 85.
(17) Miller, J.; Melius, C. *Combust. Flame* **1992**, *91*, 21.
(18) Melius, C. F.; Miller, J. A.; Evleth, E. M. *24th Symp. (Int.) Comb.* **1993**, 621.
(19) Morter, C.; Farhat, S.; Adamson, J.; Glass, G.; Curl, R. *J. Phys. Chem.* **1994**, *98*, 7029.
(20) Kern, R. D.; Chen, H.; Kiefer, J. H.; Mudipalli, P. S. *Combust. Flame* **1995**, *100*, 177.
(21) Miller, J. A.; Volponi, J. V.; Pauwels, J.-F. *Combust. Flame* **1996**, *105*, 451.
(22) Mebel, A. M.; Lin, S. H.; Yang, X. M.; Lee, Y. T. *J. Phys. Chem. A* **1997**, *101*, 6781.
(23) (a) Vereecken, L.; Pierloot, K.; Peeters, J. *J. Chem. Phys.* **1998**, *108*, 1068. (b) Vereecken, L.; Peeters, J., *J. Phys. Chem. A* **1999**, *103*, 5523.
(24) Guadagnini, R.; Schatz, G. C.; Walch, S. P. *J. Phys. Chem. A* **1998**, *102*, 5857.
(25) Jackson, W. M.; Anex, D. S.; Continetti, R. E.; Balko, B. A.; Lee, Y. T. *J. Chem. Phys.* **1991**, *95*, 7327.
(26) Deyerl, H. J.; Fischer, I.; Chen, P. *J. Chem. Phys.* **1999**, *111*, 3441.
(27) Eyring, H.; Lin, S. H.; Lin, S. M. *Basic Chemical Kinetics*; Wiley: New York, 1980.
(28) Robinson, P. J.; Holbrook, K. A. *Unimolecular Reactions*; Wiley: New York, 1972.
(29) Steinfeld, J. I.; Francisco, J. S.; Hase, W. L. *Chemical Kinetics and Dynamics*; Prentice-Hall: Englewood Cliffs, NJ, **1999**.
(30) Baer, T.; Hase, W. L. *Unimolecular Reaction Dynamics: Theory and Experiment*; Oxford University Press: Oxford, 1996.

(31) MOLPRO is a package of ab initio programs written by Werner H.-J.; Knowles P. J. with contributions from Almlöf J.; Amos R. D.; Deegan M. J. O.; Elbert S. T.; Hampel C.; Meyer W.; Peterson K.; Pitzer R.; Stone A. J.; Taylor P. R.; Lindh R.

(32) Frisch, M. J.; Trucks, G. W.; Schlegel, H. B.; Scuseria, G. E.; Robb, M. A.; Cheeseman, J. R.; Zakrzewski, V. G.; Montgomery, J. A., Jr.; Stratmann, R. E.; Burant, J. C.; Dapprich, S.; Millam, J. M.; Daniels, A. D.; Kudin, K. N.; Strain, M. C.; Farkas, O.; Tomasi, J.; Barone, V.; Cossi, M.; Cammi, R.; Mennucci, B.; Pomelli, C.; Adamo, C.; Clifford, S.; Ochterski, J.; Petersson, G. A.; Ayala, P. Y.; Cui, Q.; Morokuma, K.; Malick, D. K.; Rabuck, A. D.; Raghavachari, K.; Foresman, J. B.; Cioslowski, J.; Ortiz, J. V.; Stefanov, B. B.; Liu, G.; Liashenko, A.; Piskorz, P.; Komaromi, I.; Gomperts, R.; Martin, R. L.; Fox, D. J.; Keith, T.; Al-Laham, M. A.; Peng, C. Y.; Nanayakkara, A.; Gonzalez, C.; Challacombe, M.; Gill, P. M. W.; Johnson, B.; Chen, W.; Wong, M. W.; Andres, J. L.; Gonzalez, C.; Head-Gordon, M.; Replogle, E. S.; Pople, J. A. *GAUSSIAN 98*, *Revision A.5*, Gaussian Inc.: Pittsburgh: PA, 1998.

(33) Press, W. H.; Teukolsky, S. A.; Vetterling, W. T., Flannery, B. P. *Numerical Recipes in Fortran 77. The Art of Scientific Computing*, 2nd ed.; Cambridge University Press: Cambridge, 1992.

(34) Rubio, M.; Starling, J.; Bernhardsson, A.; Lindh, R.; Roos, B. O. *Theor. Chem. Acc.* **2000**, *105*, 15.

(35) Ochsenfeld, C.; Kaiser, R. I.; Lee, Y. T.; Suits, A. G.; Head-Gordon, M. *J. Chem. Phys.* **1997**, *106*, 4141.

(36) (a) Kaiser, R. I.; Lee, Y. T.; Suits, A. G. *J. Chem. Phys*. **1996**, *105*, 8705. (b) Le, T. N.; Lee, H.-y.; Mebel, A. M.; Kaiser, R. I. *J. Phys. Chem. A* **2001**, *105*, 1847.

(37) Seburg, R. A.; Patterson, E. V.; Stanton, J. F.; McMahon, R. J. *J. Am. Chem. Soc.* **1997**, *119*, 5847.